SCAM analysis of Panx1 suggests a peculiar pore structure

Junjie Wang and Gerhard Dahl

Department of Physiology and Biophysics, University of Miami School of Medicine, Miami, FL 33136

Vertebrates express two families of gap junction proteins: the well-characterized connexins and the pannexins. In contrast to connexins, pannexins do not appear to form gap junction channels but instead function as unpaired membrane channels. Pannexins have no sequence homology to connexins but are distantly related to the invertebrate gap junction proteins, innexins. Despite the sequence diversity, pannexins and connexins form channels with similar permeability properties and exhibit similar membrane topology, with two extracellular loops, four transmembrane (TM) segments, and cytoplasmic localization of amino and carboxy termini. To test whether the similarities extend to the pore structure of the channels, pannexin 1 (Panx1) was subjected to analysis with the substituted cysteine accessibility method (SCAM). The thiol reagents maleimidobutyryl-biocytin and 2-trimethylammonioethyl-methanethiosulfonate reacted with several cysteines positioned in the external portion of the first TM segment (TM1) and the first extracellular loop. These data suggest that portions of TM1 and the first extracellular loop line the outer part of the pore of Panx1 channels. In this aspect, the pore structures of Panx1 and connexin channels are similar. However, although the inner part of the pore is lined by amino-terminal amino acids in connexin channels, thiol modification was detected in carboxyterminal amino acids in Panx1 channels by SCAM analysis. Thus, it appears that the inner portion of the pores of Panx1 and connexin channels may be distinct.

The Journal of General Physiology

INTRODUCTION

The human genome and that of other vertebrates/deuterostomes contain two families of gap junction proteins: the well-known connexins and the pannexins. The latter were discovered based on their limited sequence homology to the innexins, the gap junction proteins of invertebrates/protostomes (Panchin et al., 2000). It has been recognized that innexins are bifunctional. In addition to their classical role as gap junction channel–forming proteins, innexins also form membrane channels for the exchange of small solutes between the extra- and intracellular spaces (Bao et al., 2007; Chuang et al., 2007). We speculate that during evolution, the gap junction function was taken over by connexins, while innexin-related pannexins were retained for the nonjunctional membrane channel function. Presently, there is no evidence that pannexins form gap junction channels in vivo (Dahl and Locovei, 2006). As glycoproteins, they even seem to be prevented from exerting this channel function (Boassa et al., 2007, 2008; Penuela et al., 2007). Instead, pannexin 1 (Panx1) appears to exclusively form nonjunctional membrane channels and serve, for example, as an ATP release channel (Dahl and Locovei, 2006; Locovei et al., 2006a; Iglesias et al., 2009; Qiu and Dahl, 2009; Ransford et al., 2009).

There is no sequence homology between connexins and pannexins or innexins (Panchin, 2005). Even the similarity between pannexins and innexins is very limited and restricted to small segments of the proteins. The sequence identity of aligned segments of various pannexins and innexins is only 25–33%, and even considering conservative substitutions, the similarity is only 36–45% (Yen and Saier, 2007). Despite the lack of sequence similarity, the channels formed by all three types of protein share several features. They form large channels with limited selectivity between cations and anions. With the exception of some differences in sensitivity, they are all affected by the same set of "gap junction blockers," including carbenoxolone (CBX), flufenamic acid, and cytoplasmic acidification (Bruzzone et al., 2005; Locovei et al., 2006b). Connexins and pannexins have similar membrane topology (Fig. 1); i.e., both types of proteins are characterized by four transmembrane (TM) segments, two extracellular loops, and cytoplasmic localization of both amino and carboxy termini (Goodenough et al., 1988; Locovei et al., 2006a). Finally, both connexin and Panx1 channels are hexameric assemblies of subunits (Boassa et al., 2007).

Considering the similarities in channel properties, the question arises whether the permeation pathways in connexin and pannexin/innexin channels are provided by similar pore structures despite the lack of similarity of primary sequence. The pore structure of connexins is now reasonably well defined. Initial attempts to identify

Correspondence to Gerhard Dahl: gdahl@miami.edu

Abbreviations used in this paper: CBX, carbenoxolone; MBB, maleimidobutyryl-biocytin; MTS, methanethiosulfonate; MTSBn, benzyl MTS; MTSES, sodium 2-sulfonatoethyl MTS; MTSET, 2-trimethylammonioethyl-MTS; Panx1, pannexin 1; PEG, polyethylene glycol; SCAM, substituted cysteine accessibility method; TM, transmembrane; wt, wild type.

The Rockefeller University Press $30.00
J. Gen. Physiol. Vol. 136 No. 5 515–527
www.jgp.org/cgi/doi/10.1085/jgp.201010440

pore-lining residues in connexin channels with the substituted cysteine accessibility method (SCAM) (Akabas et al., 1992) led to the conclusion that a portion of the first TM segment plays a critical role in the permeation pathways of Cx46 and of $Cx32E_1 43$, a chimera between Cx32 and Cx43 (Zhou et al., 1997). Domain exchange between connexins also supported a role of the extracellular portion of the first TM segment as a determinant of pore properties (Hu and Dahl, 1999; Hu et al., 2006; Ma and Dahl, 2006). The reactivity of substituted cysteines in the first extracellular loop indicated that the pore lining extends into this segment of the connexin protein (Kronengold et al., 2003).

Recently, the structure of the Cx26 gap junction channel at 3.5-Å resolution has been published (Maeda et al., 2009). The crystal structure confirms the contribution of the external portion of the first TM segment and the first extracellular loop moieties as pore-lining entities. The atomic structure further identifies the amino terminus as the remaining pore-lining segment in the inner portion (toward the cytoplasm) of the channel.

Here, we apply SCAM to identify pore-lining residues in Panx1. The data indicate that pannexin and connexin channels share some aspects but are quite dissimilar in others. The contribution of the first TM segment and the extracellular loop moieties is common to both channels, whereas in pannexin channels, the inner aspect of the pore is determined by the carboxyterminus.

MATERIALS AND METHODS

Materials

Mouse Panx1 was provided by R. Dermietzel (University of Bochum, Bochum, Germany). The thiol reagent maleimidobutyryl-biocytin (MBB) was purchased from EMD. MBB was dissolved in DMSO to a stock concentration of 100 mM. Pyrenyl maleimide, benzyl methanethiosulfonate (MTSBn), 2-trimethylammonioethyl-methanethiosulfonate (MTSET), and sodium 2-sulfonatoethyl methanethiosulfonate (MTSES) were purchased from Toronto Research Chemicals. MTSET and MTSES were dissolved in distilled water to a stock concentration of 100 mM, and aliquots were stored at −20°C. For experiments, an aliquot was diluted in OR2 to the concentration of 1 mM and used immediately.

Mutagenesis

Site-directed mutations were generated according to the protocol of the QuikChange II Site-Directed Mutagenesis kit (Agilent Technologies). Mutant plasmids were transformed into competent *Escherichia coli* cells by heat shock. Transformed cells were grown in LB agar plate with ampicillin at 37°C for 16 h. Individual colonies were picked from selective plates and grown in LB media with antibiotic for 16 h. The mutation plasmid was purified from *E. Coli* cells according to the protocol of QIAprep Spin Miniprep kit (QIAGEN). Purified mutation plasmids were sequenced by Genewiz. Panx1, in pCS2, was linearized with NotI. In vitro transcription was performed with SP6 Message Machine kit (Applied Biosystems). mRNAs were quantified by absorbance (260 nm), and the proportion of full-length transcripts was checked by agarose gel electrophoresis. In vitro–transcribed mRNAs (~40 nl) were injected into *Xenopus laevis* oocytes.

Preparation of oocytes

All procedures were conduced in accordance with the Guiding Principles for Research Involving Animals and Human Beings of American Physiological Society. Preparation of oocytes was performed as described previously (Dahl, 1992). Ovaries of *Xenopus* were cut into small pieces and incubated in 2.5 mg/ml of collagenase (Worthington) calcium-free OR2 solution, stirring at one turn/second at room temperature. Typically, the incubation period was 3 h for oocytes to be separated from the follicle cells. Extensive washing by regular OR2 followed, and healthy-looking oocytes were selected for mRNA expression. Optimal oocytes were in the final stage of maturity with a diameter of 1–1.2 mm and with even pigmentation.

Electrophysiological techniques

After injection of mRNA, the oocytes were incubated at 18°C for 24–48 h in oocyte Ringer's solution (in mM): 82.5 NaCl, 2.5 KCl, 1 $MgCl_2$, 1 $CaCl_2$, 1 Na_2HPO_4, and 5 HEPES, pH 7.5. Whole cell membrane current of single oocyte was measured using a two-microelectrode voltage clamp (Geneclamp 500B; Axon Instruments) and recorded with a chart recorder (SOLTEC). Both voltage-measuring and current-passing microelectrodes were pulled with a flaming/brown micropipette puller (P-97; Sutter Instrument Co.) and filled with 3 M KCl. The recording chamber was perfused continuously with solution. Membrane conductance was determined using voltage pulses. Oocytes expressing Panx1 were held at −60 mV, and pulses lasting 5 s to +20 or +60 mV were applied to transiently open the channels. The thiol reagents were applied by perfusion of the oocyte chamber and were administered until a steady-state level of currents was reached.

Data analysis

To determine percent inhibition of membrane currents, lines were drawn on enlarged records through peak currents before and after the application of the thiol reagent. The same was done at the baseline to account for eventual baseline shifts. Percent inhibition was calculated. The time constant (τ) was determined graphically, and the reaction rate (R) was calculated according to: $R = 1/\tau \times [M]$, where M is the concentration of the thiol reagent. The statistical significance of the differences between the means was tested by one-way ANOVA, followed by Dunnett's test. In all figures, statistical significance is indicated as follows: **, $P < 0.01$; *, $P < 0.05$; not significant, $P > 0.05$.

ATP release

ATP flux was determined by luminometry. Oocytes, 2 d after injection of Panx1 messenger RNA, were untreated (negative control) or stimulated with 150 mM KGlu solutions (positive control). To test the effect of MBB, oocytes were preincubated with MBB in OR2 or in KGlu. Subsequently, oocytes were stimulated with KGlu solution for 10 min. For reference to the MBB-treated samples, oocytes were preincubated with KGlu and then transferred to fresh KGlu for ATP release measurement. The supernatants were collected and assayed with luciferase/luciferin (Promega).

Online supplemental material

Fig. S1 summarizes the SCAM data obtained with MBB and MTSET for cysteine mutants of the first TM segment of Panx1. Fig. S2 shows original records of the effects of MBB and MTSET on mutants G61C and T62C. Reversible and irreversible components of the thiol reactions are apparent. Also, the different time courses of effects induced by MBB and MTSET are shown. Figs. S1 and S2 are available at http://www.jgp.org/cgi/content/full/jgp.201010440/DC1.

RESULTS

Although originally discovered as a gap junction protein, Panx1 does not seem to form the cell-to-cell channels of gap junctions. Instead, this protein appears to exclusively

function as a channel in the nonjunctional membrane, allowing the exchange of molecules between the cytoplasm and the extracellular space. Thus, in contrast to the cell-to-cell channels formed by most gap junction proteins, the Panx1 channels are directly accessible from the extracellular space and therefore can be analyzed by SCAM. Panx1 channels can be activated at the resting membrane potential by mechanical stress (Bao et al., 2004), by ATP through purinergic receptors (Locovei et al., 2006b, 2007), and by potassium ions (Silverman et al., 2009), consistent with their role as ATP release channels. They can also be activated by voltage (Bruzzone et al., 2003). However, the voltages required for channel opening are in the positive voltage range; thus, voltage gating is unlikely to represent a physiological process. Nevertheless, opening of the Panx1 channels by voltage is a convenient experimental procedure, and we used this protocol for the SCAM analysis of the channels. Panx1 channels exhibit multiple conductance states (Bao et al., 2004), diminishing the interpretive advantages of single-channel recordings. Therefore, for this study, we relied on whole cell membrane currents.

The Panx1 sequence contains 10 cysteines. Four of them are the signature cysteines of pannexins and innexins in the extracellular loops (Fig. 1). To test whether any one of the endogenous cysteines is reactive to thiol reagents, wild-type (wt) mouse Panx1 was expressed in *Xenopus* oocytes, and channel activity was determined by two-electrode voltage clamp. Membrane currents were induced by voltage steps from a holding potential of −60 to +60 mV. Extracellular application of 100 µM MBB (mol wt, 537) resulted in attenuation of Panx1 currents (Fig. 2 A). Although MBB is known to react with a thiol group forming an irreversible covalent bond, part of the current inhibition reversed upon washout of the compound. A second application of MBB again attenuated the currents and did so reversibly, leaving the same irreversible component of current inhibition. Thus, MBB exerted two effects on wt Panx1. The irreversible component indicated that at least one of the endogenous cysteines reacted with MBB and, baring gating effects, was sufficiently close to the permeation pore to affect membrane conductance. The reversible component probably is a steric effect from the partitioning of free MBB in the channel, as indicated by a similar reversible current inhibition by polyethylene glycols (PEGs) in the same size range (PEG400 and PEG600), as shown in Fig. 2 B. As shown later, other thiol reagents (methanethiosulfonates [MTS]) also exhibited a reversible and an irreversible component of current inhibition. Consistent with a steric effect responsible for the reversible component, these smaller compounds attenuated the currents less.

Replacement of the endogenous cysteines by serine residues individually resulted in complete loss of channel activity for all four extracellular cysteines, consistent with the conserved nature of these cysteines. Oocytes expressing the replacement mutants C40S and C346S died soon after injection of the respective mRNAs. Cell death was prevented by incubating the cells with 100 µM CBX, an unspecific blocker of pannexin channels (Fig. 3). Five out of eight cells injected with Panx1 C40S were dead within 24 h, as compared with none out of seven oocytes incubated with CBX. The comparable numbers for Panx1 C346S were 6/7 without and 0/10 with CBX. Removal of the drug under voltage clamp conditions resulted in the development of membrane currents that were susceptible to CBX inhibition. These observations suggest that in contrast to wt Panx1, the cysteine replacement mutants C40S and C346S form channels that exhibit a substantial open probability at the resting membrane potential.

The cysteine replacement mutants C136S, C215S, C227S, and C426S formed channels with similar basic properties as wt Panx1. With the exception of the increased open probability at the resting membrane potential, this was also the case for mutants C40S and C346S. The application of 100 µM MBB resulted in the same two-component response as in wt Panx1 channels, except in the C426S mutant–expressing oocytes, where only the reversible component was observed (Fig. 2, C and D). Thus, the irreversible thiol reaction has to be attributed to this carboxyterminal cysteine. Consequently, all mutants for the SCAM analysis were based on Panx1 C426S. For simplicity, however, only the cysteine replacing an endogenous amino acid will be identified in the mutants used in the SCAM analysis. For example, the mutant Panx1 T62C,C426S is termed Panx1 T62C or T62C for short.

Of the 115 mutants generated for the SCAM analysis, 25 did not yield channel activity (Fig. 1 B). The remaining 90 mutants formed membrane channels, which could be blocked by CBX, consistent with their formation by the Panx1 mutants. The gating by membrane voltage of these mutant channels was similar to that of wt Panx1 channels.

The current inhibition by MBB observed in wt Panx1 and some SCAM mutants could be from steric block of the thiol reagents present in the permeation pathway or a gating process. Typically, single-channel analysis allows discrimination between these possibilities. Indeed, the thiol reaction with engineered cysteins can be resolved in connexin channels by single-channel analysis (Pfahnl and Dahl, 1998). An elegant study used this approach for an extensive cysteine scan of Cx46 and demonstrated multiple transitions of channel conductance consistent with successive reactions of the cysteines in individual subunits (Kronengold et al., 2003). The properties of Panx1 channels, however, are not conducive for single-channel analysis of the thiol reaction. The channel exhibits multiple subconductance states that, at least at

present, cannot be experimentally controlled. The application of this analysis in previous attempts failed to discriminate between the blocking and gating actions of various drugs (Qiu and Dahl, 2009). Because of the complexity of the subconductance states, it could not be discerned whether the drugs forced the channel into some of the subconductance states or whether channel conductance was attenuated. Consequently, in the present study, the cysteine mutants were analyzed on the basis of macroscopic currents obtained by two-electrode voltage clamp.

Of the cysteine substitution mutants in the first TM segment TM1, I50C, S51C, L52C, A53C, Q56C, E57C, Q63C, and I64C failed to form the voltage-gated channels typical for Panx1. MBB was applied to functional mutants and caused substantial inhibition at positions F54C,

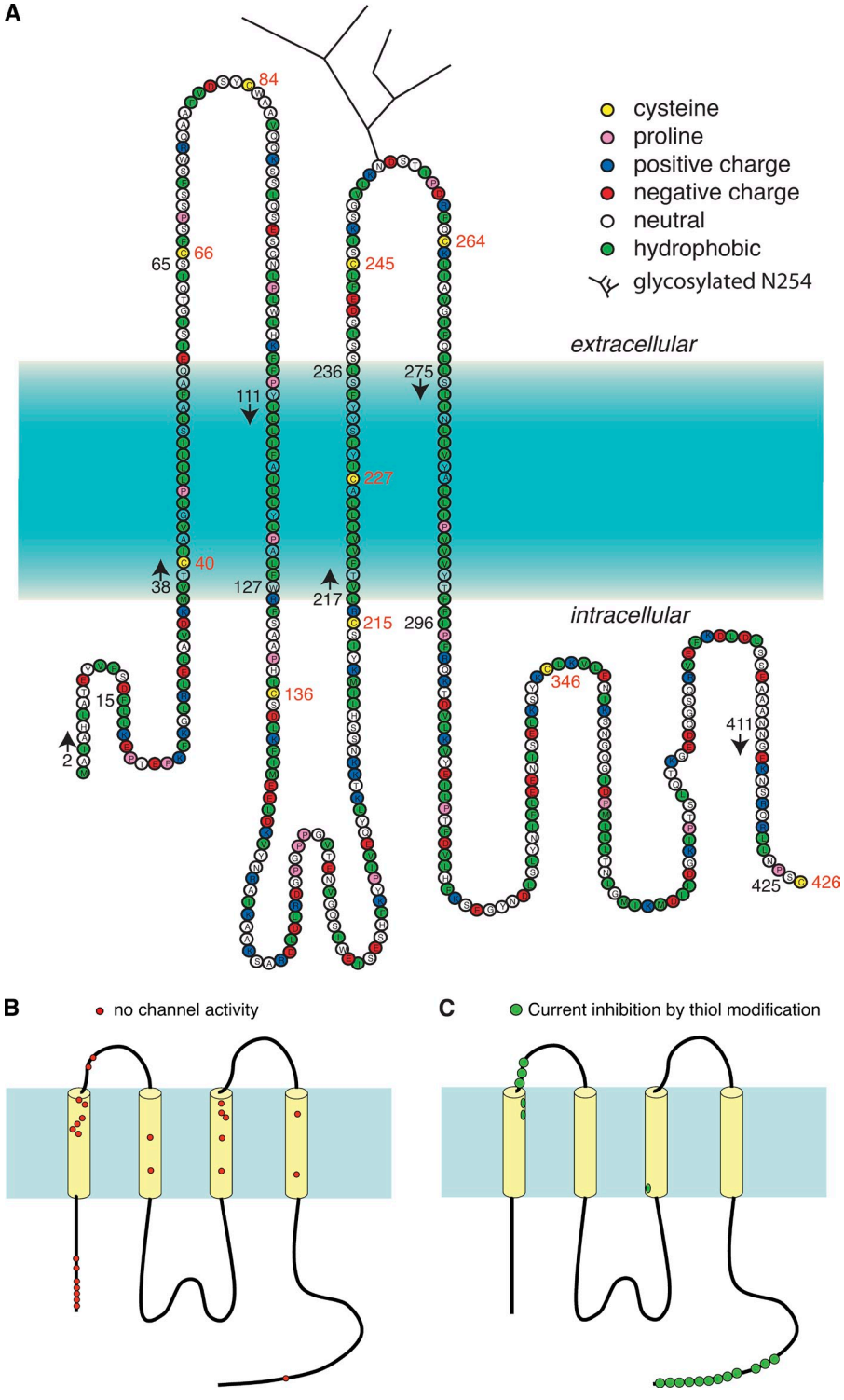

Figure 1. Topology of mouse Panx1 based on hydrophobicity plots, site-specific antibodies, and glycosylation analysis (Locovei et al., 2006a; Boassa et al., 2007). (A) The topology of Panx1 in the membrane appears to be similar to that of connexins, with four predicted TM segments, two extracellular loops, and cytoplasmic localization of the amino and carboxy termini (Locovei et al., 2006a; Boassa et al., 2007; Penuela et al., 2007). Based on hydrophobicity analysis by the software programs TMpred, TMHMM, and DNA Star, the following boundaries for the TM segments are predicted: M38-I60 for TM1, F108-W127 for TM2, L217-236 for TM3, and L275-I296 for TM4. Because of uncertainty of the predictors, the boundaries in the figure are represented by a color gradient. Positions of endogenous cysteines are indicated with red numbers. The beginning (arrows) and end of stretches of amino acids substituted by cysteines for SCAM analysis are indicated by black numbers. (B) Localization of Panx1 SCAM mutants not forming functional channels. Clusters of these mutants are in the amino terminus, the first TM segment, and the third TM segment, indicating a structural importance of these moieties. (C) Positions of modified cysteines.

I60C, G61C, and T62C (Figs. 4 and 5, and Fig. S2). As observed for wt Panx1 channels, the MBB reaction was twofold, including a reversible and an irreversible component. The reversible component was strictly dose dependent and was obvious at 100 µM but barely detectable at 10 µM MBB. The second component exhibited strong dose dependency for the rate of inhibition (Fig. 4 and Table I).

Residue substitution in the remaining three TM segments, M2, M3, and M4, by cysteine was in general well tolerated. With the exception of mutants L115C and Y121C in TM2, I223C, Y229C, Y232C, Y233C, and S235C in TM3, and N279C and V291C in TM4, all other mutants formed the voltage-gated channels typical for Panx1. MBB applied to the channel-forming mutants remained without any significant irreversible effect on membrane currents (Fig. 5). The transient small inhibition of the currents, however, was observed in all mutant channels, consistent with an effect unrelated to thiol groups.

All reactive cysteines in the SCAM analysis of Panx1 channels are located in the external half of TM1 and extend into the first extracellular loop (Fig. 5). Thus, the cytoplasmic aspect of the channel was missed either because it is not formed by TM segments or because of the choice of MBB as thiol reagent. Considering the large size of the Panx1 channel with 500-pS single-channel conductance (Bao et al., 2004) and its accessibility to PEGs up to the size of PEG1500 (Wang et al., 2007), it is unlikely that MBB (mol wt, 537) is excluded from the narrow part of the channel. Nevertheless, the SCAM analysis of the TM segments was repeated with the smaller thiol MTS reagent, MTSET (mol wt, 278). The molecular dimensions (largest abaxial diameter) of the compounds are 1.1 nm for MBB (determined with Chem3D/MOPAC analysis) and 0.6 nm for MTSES and MTSET (Kaplan et al., 2000). The opposite charge (positive) of MTSET as compared with the negatively charged MBB allowed for testing charge effects in addition to the difference in size. All reactive cysteines can be expected to be exposed to water because only the ionized cysteine SH group will react with the thiol reagents, and ionization requires water exposure. Consequently, cysteines in bona fide TM segments should only be susceptible for modification by thiol reagents if they are accessible from the channel pore. Only if water-filled crevices existed in Panx1 that were sufficiently large to accommodate thiol reagents would a change in membrane currents caused by thiol modification not indicate a pore-lining position. For the thiol reagents used in this study, specifically MBB, such false positive results are unlikely.

As shown in Fig. 6 and Fig. S1, the reactive sites in TM1 for MTSET matched those identified with MBB as thiol reagent. However, MTSET also revealed two additional

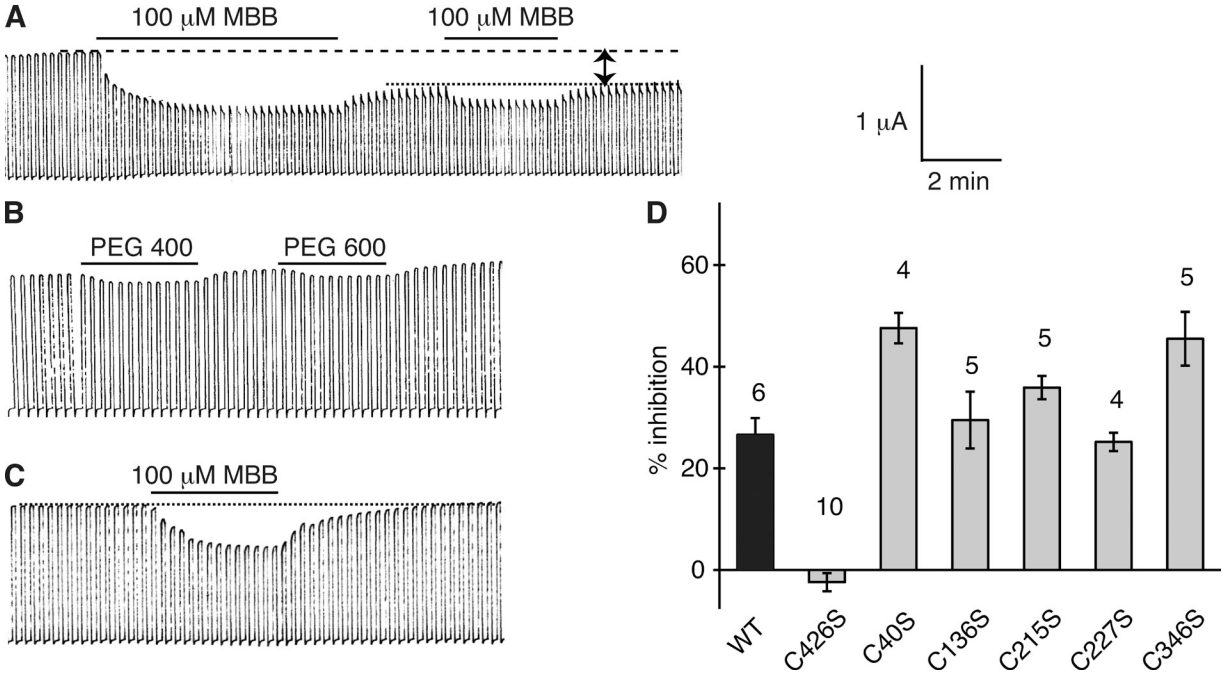

Figure 2. Membrane currents induced by voltage steps from −60 to +60 mV at a rate of five/minute in oocytes expressing wt Panx1 (A and B) or Panx1 C426S. (A) 100 µM MBB induced a twofold response in wt Panx1 channels consisting of a reversible and an irreversible component (arrows). The reversible component was inducible by a subsequent application of MBB. The irreversible component was used to assess channel inhibition in all subsequent figures. (B) PEG400 and PEG600 at 1 mM caused a similar reversible channel inhibition as MBB. (C) 100 µM MBB applied to Panx1 C426S channels exclusively caused the reversible inhibition. (D) Quantitative analysis of irreversible inhibition of membrane currents by 100 µM MBB in oocytes expressing wt Panx1 and its cysteine replacement mutants C426S, C40S, C136S, C215S, C227S, and C346S.

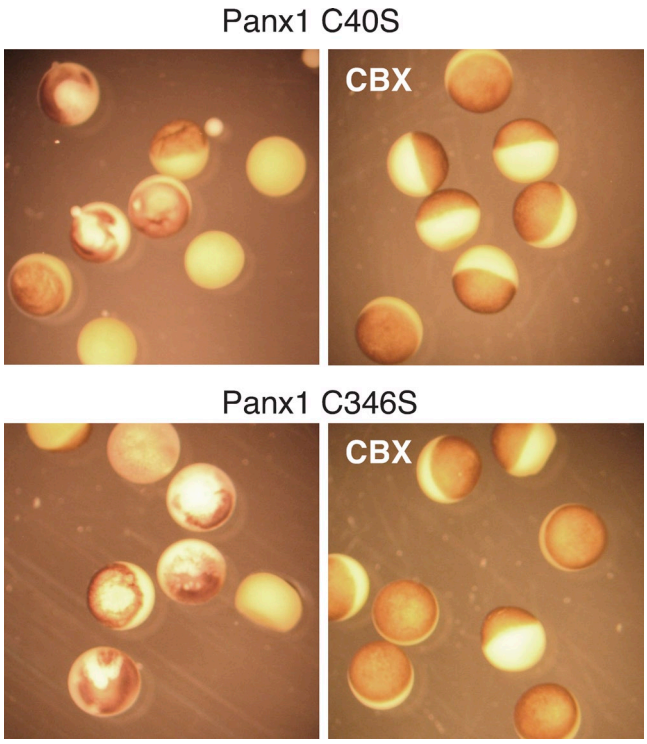

Figure 3. Micrographs of oocytes expressing Panx1 C40S or Panx1 C346S (top and bottom) incubated in OR2 medium (left) or in OR2 with 100 μM CBX (right). Pictures were taken 20 h after injection of mRNA.

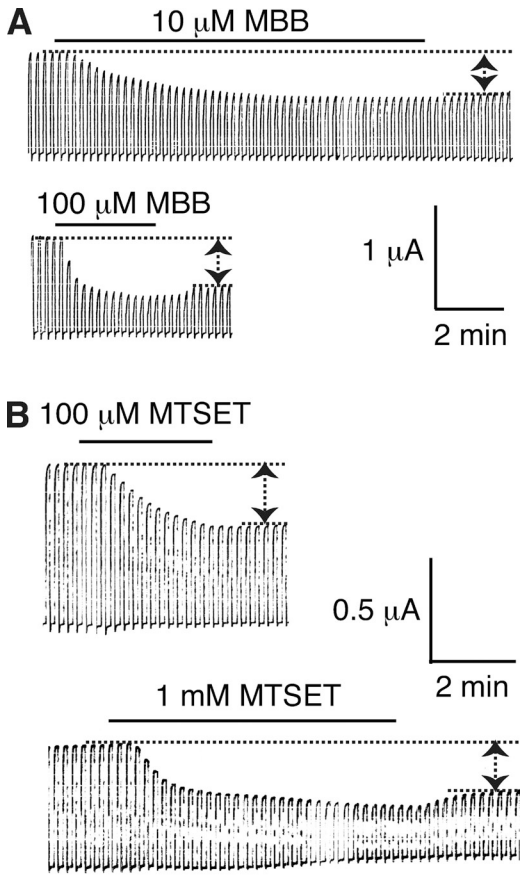

Figure 4. Dose-dependent modification of engineered cysteines in Panx1 by MBB (A) or MTSET (B). Membrane currents of oocytes expressing Panx1 I60C were attenuated by 10 or 100 μM MBB and by 100 μM or 1 mM MTSET. Both components, the reversible and the irreversible inhibition of the currents, were affected in a dose-dependent way. The reversible component was barely detectable at the lower MBB or MTSET concentrations.

reactive sites: I58C, which was already suspect in the MBB scan, and S59C. Like MBB, MTSET did not identify reactive sites in segments TM2 and TM4. In TM3, the mutant L217C treated with 1 mM MTSET exhibited marginal inhibition of the currents (Fig. 6). Surprisingly, the apparent reaction rates for MTSET were slower than that observed for MBB, as shown for the I60C mutant (Table I). This contradicts the reactivity of these reagents with freely accessible thiol groups, where MTSET reacts considerably faster than MBB. It is conceivable that the slower apparent reaction rate of MTSET reflects a complex reaction pattern, where reactions with individual subunits may not be independent. Instead, reaction with one subunit may affect the accessibility and reaction rates with other subunits, so that reactions are progressively impeded. On the other hand, MBB may be able to react with only few, if not only one, subunit of a channel.

Although in most positions the effects of MBB and MTSET matched qualitatively, there was one major

TABLE I

Time constants (τ) and apparent modification rates (R) for current attenuation by MBB and MTSET in wt Panx1 and Panx1 I60C, C426S channels

Parameter	Channel	10 μM MBB	100 μM MBB	100 μM MTSET	1 mM MTSET
τ (s)					
	wt Panx1		28.5 ± 1.5 (4)		
	Panx1 I60C	129 ± 12.4 (4)	26.4 ± 4.1 (5)	164 ± 8 (3)	60 ± 9.8 (4)
R ($M^{-1}s^{-1}$)					
	wt Panx1		351		
	Panx1 I60C	775	378	61	17

Means ± SE and the number of oocytes analyzed are given. The τ's for wt Panx1 and I60C were not significantly different. Significant differences ($P > 0.05$) were found between the means for 10 and 100 μM MBB and between 100 μM and 1 mM MTSET. The means for MBB and MTSET each at 100 μM were also significantly different.

discrepancy. The two thiol reagents resulted in opposite effects in the mutant F54C. MTSET, after a very brief diminution of the currents, caused an amplification of the currents, which was reversed by subsequent reduction with dithiothreitol. To test whether this discrepancy was attributable to the opposite charges of the two compounds, a negatively charged (MTSES) and a neutral (MTSBn) MTS were used. Both MTSES and MTSBn yielded the amplification of currents as observed with MTSET (Fig. 7). In some records, the amplification followed a brief period of current diminution. To test whether the different chemical bonds created by maleimide and MTS reagents were at the root of the opposite effects on membrane currents of the F54C mutant, a neutral maleimide in the same size range as the MTS reagents (pyrenylmaleimide: mol wt, 297) was tested. As shown in Fig. 7, this smaller maleimide yielded the same amplification of F54C currents as the MTS reagents. Thus, size rather than charge or chemical bond appears to matter in determining whether inhibition (MBB: mol wt, 537) or amplification (MTSET: mol wt, 278; MTSES: mol wt, 233; MTSBn: mol wt, 202; pyrenyl maleimide: mol wt, 297) resulted from application to the F54C mutant.

The rescan of the TM segments with MTSET as thiol reagent failed to identify the missing cytoplasmic portion of the channel pore. Although current inhibition was observed with this compound in one position (L217C) in the cytoplasmic aspect of TM3, the effect was low (15% inhibition), and the single reactive site is probably not sufficient to account for all of the missing pore lining. The crystal structure of Cx26 revealed that amino-terminal amino acids line the pore at the cytoplasmic half of the channel (Maeda et al., 2009). Consequently, amino-terminal acids in Panx1 were substituted by cysteines and subjected to SCAM analysis. Only a few mutants generated functional channels, and they all were unresponsive to the application of 100 μM MBB (Fig. 8). An extraordinary number of amino-terminal mutants failed to yield active channels. This suggests that, regardless of the mechanism of failure, the amino terminus is critical for proper folding of Panx1. This may affect the channel's initial transfer and

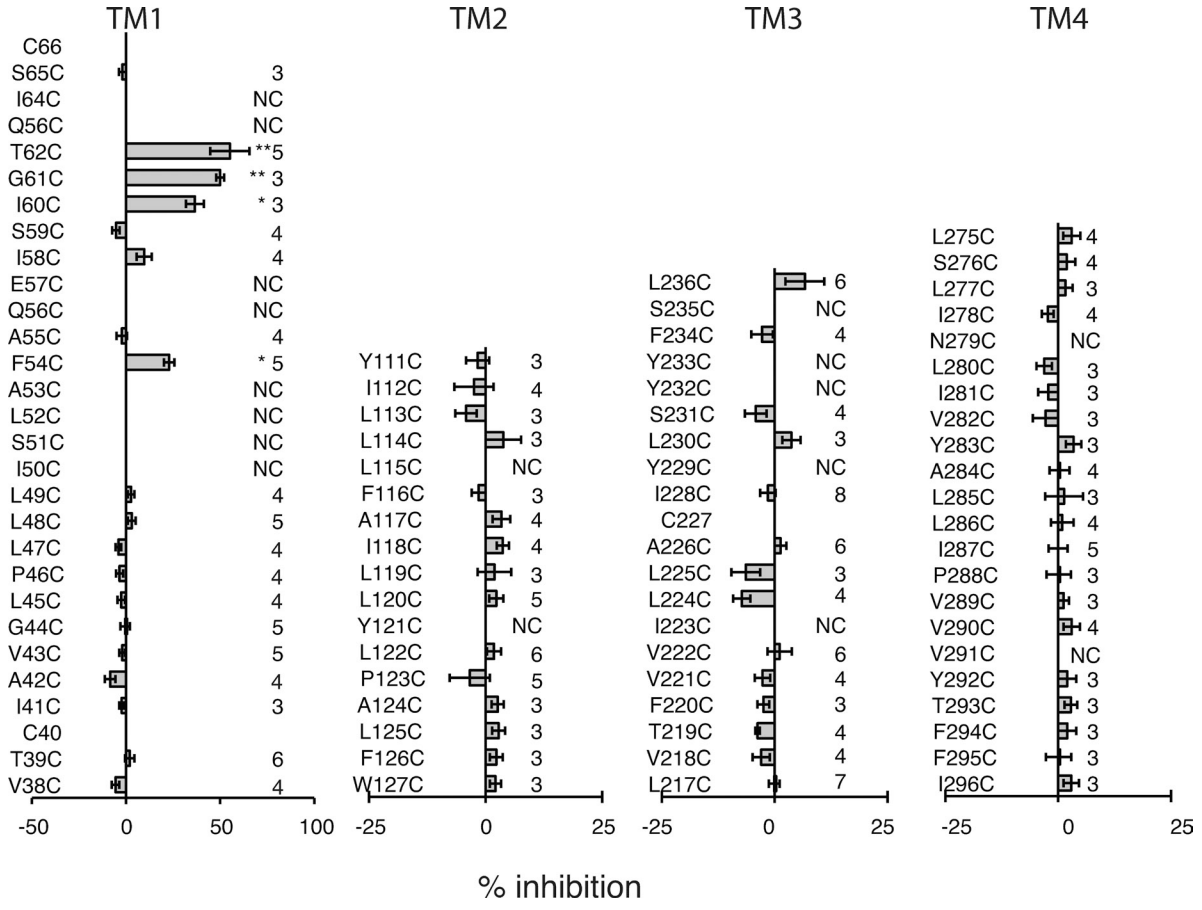

Figure 5. SCAM analysis of the four TM segments of Panx1, with MBB as thiol reagent. The amino acids are arranged in ascending order for TM1 and TM3 and in descending order for TM2 and TM4 to reflect their directional orientation in the membrane. Means ± SE of irreversible current inhibition by 100 μM MBB are plotted. The number of oocytes analyzed is indicated on the right. NC, no channel activity was detected. *, $P < 0.05$; **, $P < 0.01$ (vs. Panx1 C426S control).

folding in the ER, and shuttling or functionality in the plasma membrane.

Our initial experiments identified the carboxyterminal cysteine of wt Panx1 to be reactive for thiol reagents, as indicated by the attenuation of membrane currents after the application of such reagents. It was therefore of interest whether adjacent amino acids have a similar exposure to the permeation pathway. Consequently, the SCAM analysis was extended to the 15 carboxyterminal amino acid positions. However, several reactive sites were found that exhibit an unprecedented pattern. Reactivity was observed in nine consecutive positions (Fig. 8). Only one mutant in the carboxyterminal segment, S417C, failed to form patent channels. As shown for the terminal cysteine in wt Panx1, the apparent reaction rate was similar to that observed for the I60C mutant (Table I), suggesting a similar mode of access.

The accessibility of MBB to two representative positions in TM1/E1 and the carboxyterminus, T62C and C426, was retested with an independent assay. Upon stimulation with K^+, uninjected oocytes release ATP, probably by a vesicular mechanism, as indicated by the sensitivity to brefeldin (Maroto and Hamill, 2001). Expression of Panx1 in oocytes results in a 10-fold higher K^+-induced ATP release, which can be blocked by Panx1 channel inhibitors (Bao et al., 2004; Silverman et al., 2008; Qiu and Dahl, 2009). As shown in Fig. 9, preincubation with MBB inhibited ATP release in oocytes expressing wt Panx1 and Panx1 T62C. The inhibition was prominent if the oocytes were preincubated with MBB in the presence of increased extracellular K^+, which opens Panx1 channels (Silverman et al., 2009), suggesting that for reaction with the endogenous cysteine C426 or with the engineered cysteine T62C, the Panx1 channel needs to be open, making substantial membrane permeation of MBB in the experimental timeframe unlikely. The observation that the inhibition of ATP release by MBB appears to be more pronounced than the inhibition of currents is consistent with a partial block of the permeation pathway after the thiol reaction.

DISCUSSION

These results suggest that channels formed by Panx1 and by connexins share important aspects of the permeation pathway despite the absence of similarities in primary sequence. On the other hand, distinct structural features of the two channel types are also suggested by the Panx1 SCAM analysis. The similarities relate to the external portion of the channels, where the Panx1 cysteine scan identified reactive sites with a pattern similar to the pore-lining residues revealed in the crystal structure

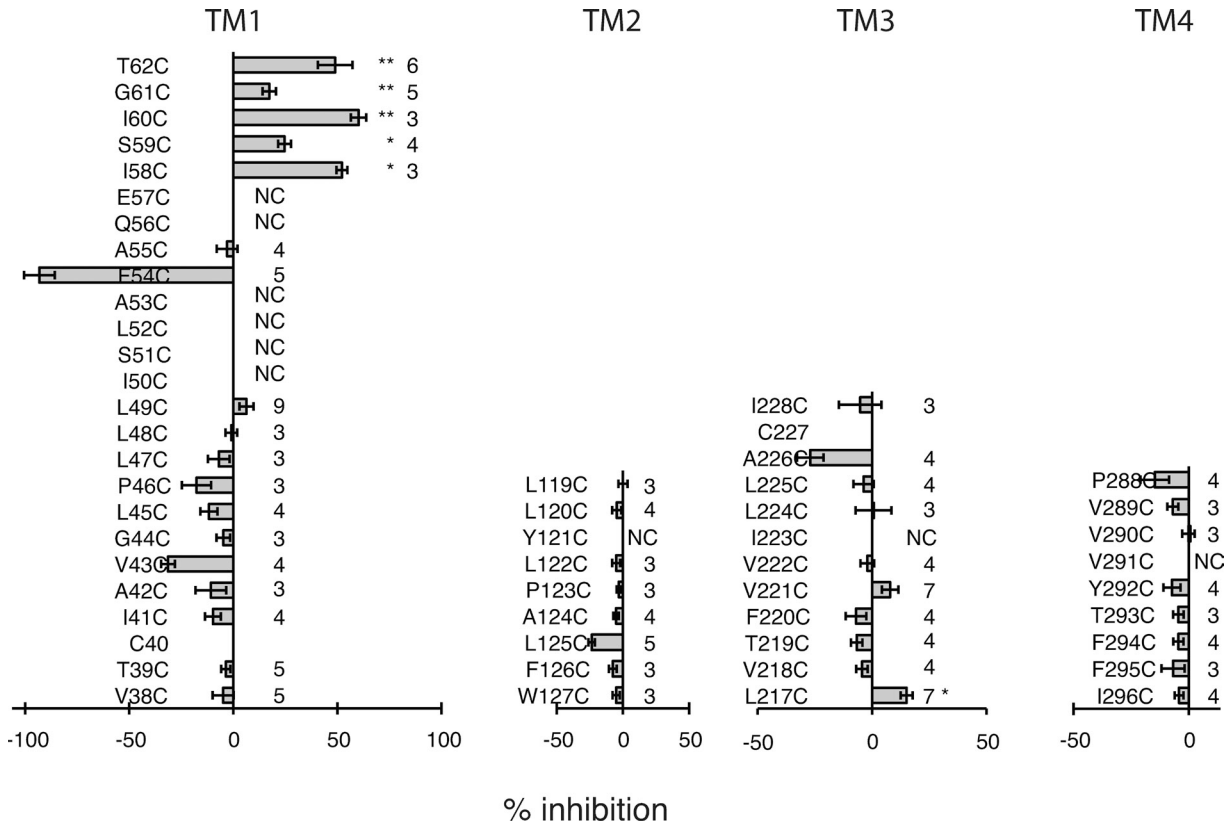

Figure 6. SCAM analysis of the four TM segments of Panx1, with MTSET as thiol reagent. Conditions were the same as described in Fig. 5, except that 1 mM MTSET was used as thiol reagent.

of Cx26 (Maeda et al., 2009). In both types of channels, this portion of the permeation pathway is constructed by amino acids in the TM segment TM1 and by portions of the first extracellular loop. The differences are in the internal portion, which is provided by amino-terminal amino acids in the Cx26 structure, whereas reactivity of carboxyterminal amino acids in Panx1 suggests a contribution of this segment to the permeation pathway.

Originally, it had been speculated that based on its amphipathic nature, the third TM segment of connexins would exclusively provide the pore of gap junction channels (Unwin, 1989; Bennett et al., 1991). Early cysteine scans of connexins in their "hemichannel" configuration did not support this notion, except that a minor contribution of TM3 could be tentatively inferred (Zhou et al., 1997). However, experiments on complete gap junction channels with the cut-open paired oocyte assay were interpreted as supporting an exclusively TM3 pore-lining function (Skerrett et al., 2002). Taken at face value, the apparent difference in pore-lining residues in gap junction hemichannels, i.e., connexons, and complete gap junction channels would suggest that upon docking, the paired connexons undergo a major conformational change, so that TM3 instead of TM1 becomes the pore-lining segment. Such a mechanism is unappealing for three reasons: (1) the permeability and gating properties of connexons and gap junction channels are very similar, if not identical; (2) the single-channel conductances of unpaired connexon channels are exactly twice that of gap junction channels, as expected from the serial arrangement of connexons in the gap junction; and (3) the crystal structure of Cx26 shows the connexons in a docked configuration, suggesting that the pore structure is that of the gap junction channel. Because the external pore lining in the crystals is similar to that predicted by cysteine scans of connexon channels, a difference in the pore structure between unpaired and paired connexons appears unlikely. However, it cannot be excluded that the crystal structure does not reflect the native docked state but captures an artifactual docking occurring during the crystallization process. If that were the case, the crystal structure would falsely identify the residues involved in the docking between two hemichannels to form the complete gap junction channel.

Modification of introduced cysteines in TM1 was limited in Panx1 channels, like in connexons to the external part of the segment. Thus, other portions of the protein need to contribute to the remainder of the TM pore. Intriguingly, limited cysteine reactivity was found in connexon channels in the internal portion of TM3 (Zhou et al., 1997). A similar pattern was also observed for Panx1 channels, although very weak and only with MTSET but not MBB. The crystal structure of Cx26 excludes a significant pore-lining function of TM3, although a limited contribution to the cytoplasmic vestibulum is possible.

The previous SCAM analyses of connexins (Zhou et al., 1997; Skerrett et al., 2002; Kronengold et al., 2003) did not systematically test "cytoplasmic" segments of the proteins, and the contribution of the amino-terminal amino acids to the permeation pathway indicated by the Cx26 crystal data was missed, except that reactivity of a cysteine mutant of the connexin chimera Cx32*43E1 T8C has been demonstrated (Oh et al., 2008). The pannexin SCAM of the 15 amino-terminal amino acids did not yield modified sites. Instead, such reactivity was found for a series of carboxyterminal amino acids.

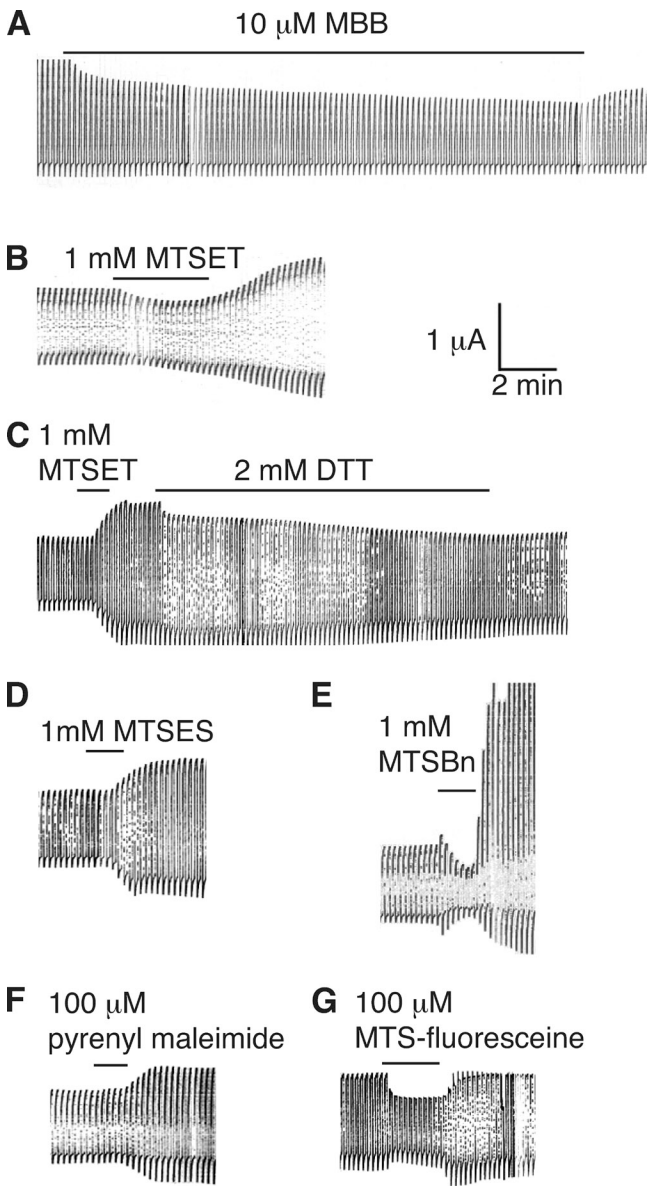

Figure 7. Effects of various thiol reagents on Panx1 F54C currents. Oocytes expressing Panx1 F54C were held at −60 mV and pulses to +60 (A) or +20 mV (B–E) were applied to activate the channel. To test for cysteine accessibility, 10 μM MBB (A), 1 mM MTSET (B), 1 mM MTSET followed by 2 mM dithiothreitol (DTT; C), 1 mM MTSES (D), 1 mM MTSBn (E), 100 μM pyrenyl maleimide (F), or 100 μM MTS-fluorescein (G) was applied.

The findings suggest that connexins and pannexins follow a very similar blueprint for channel formation, yet with differences in details. Such differences are not unexpected, as the Panx1 channel is distinct from all connexin channels in terms of permeability and gating. The Panx1 channel allows for the transit of larger molecules, has a considerably higher single-channel conductance of ~500 pS, and is characterized by multiple subconductance states (Bao et al., 2004). These subconductance states, in contrast to the mostly single subconductance states in connexin channels (Trexler et al., 1996), do not seem to be induced by voltage gradients because they appear over a wide range of voltages.

In connexins, the removal of large fragments of the carboxyterminus typically is well tolerated, and basic channel function is not impaired (Rabadan-Diehl et al., 1994). pH gating can be altered and restored by the reintroduction of the missing fragment as a separate entity (Delmar et al., 2004). These observations are consistent with a connexin pore structure not involving carboxyterminal sequences. Similar truncation studies on Panx1 have not yet been performed but could be informative about the contribution of the carboxyterminus to the channel pore formed by this protein, as indicated by the SCAM data presented here. The reactive sites in the carboxyterminus of Panx1 have an unusual pattern; they are consecutive over a stretch of amino acids instead of exhibiting the typical periodicity seen in structured protein domains. Consecutive reactive sites have also been observed in aquaporins (Shi and Verkman, 1996). However, although the stretch of amino acids in aquaporins covers four consecutive amino acids, it extends over a considerably larger range in Panx1, where a segment of nine consecutive reactive sites was observed. It cannot be excluded that this is the consequence of mutation artifacts. The cysteine replacements in this region might alter the structure so that accessibility migrates along this segment and thus does not reflect a periodicity native to the wt structure. On the other hand, the carboxyterminus of Panx1 could be unstructured and highly flexible, and in this way, amino acids may sporadically become part of the permeation pathway. Consequently, cysteines replacing the endogenous amino acids would be reactive in an ostensibly consecutive pattern. The multiplicity of subconductance states and the stochastic nature of the channel jumping between these states are consistent with a dynamic permeation pathway structure.

Two thiol reagents were used in this study, MBB and MTSET, to test reactivity of the engineered cysteines. With the exception of one position in TM1, the results with both reagents for the most part were qualitatively identical, although the reagents differ in charge and size. The cysteine replacing F54, however, yielded opposite results. MBB inhibited and MTSET enhanced conductance. Enhancement of currents by MTS reagents has been observed previously, for example, by MTSEA in the acetylcholine receptor (Zhang and Karlin, 1997). In Panx1 channels, this effect is not attributable to the difference in charge between the thiol reagents because negatively charged and neutral MTS reagents also enhanced conductance. The chemical nature of the thiol reaction also does not appear to matter, as pyrenyl maleimide had effects opposite to MBB. The common denominator of the reagents enhancing channel conductance is their considerably smaller size as compared with MBB. It appears that

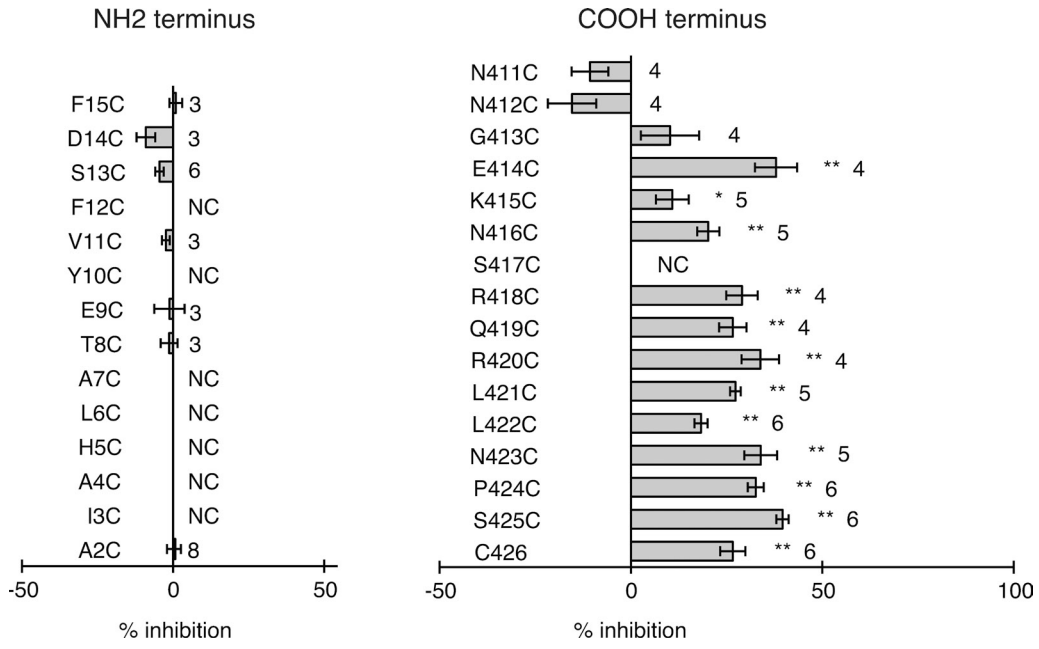

Figure 8. SCAM analysis of NH_2 and C terminus of Panx1. Conditions were the same as described in Fig. 5.

the thiol reagents, with the exception of MBB, stabilize the channel in an open state. MBB may do the same, but because of the larger size, it also impairs permeation sterically. It is also feasible that the smaller thiol reagents enter a crevice and react with an endogenous cysteine, such as C227. In this scenario, the F54C mutation would need to be responsible for creating or giving access to such a crevice. The reactivity of MTSET with the thiol group of a cysteine is very high, and it has been argued that the reagent reacts with minor channel conformations and modifies cysteines partially buried in the crevices of proteins, in addition to the freely accessible cysteines on the surface of proteins (Lü and Miller, 1995; Holmgren et al., 1996; Liu et al., 1996). Intriguingly, in many records with the small thiol reagents on F54C, a brief inhibition of channel conductance preceded the enhancement of conductance, as if the thiol reagent reacted first with F54C before reacting with an endogenous cysteine in a crevice. This reaction then could increase the membrane currents by freezing the channels in an open state and/or high conductance conformation.

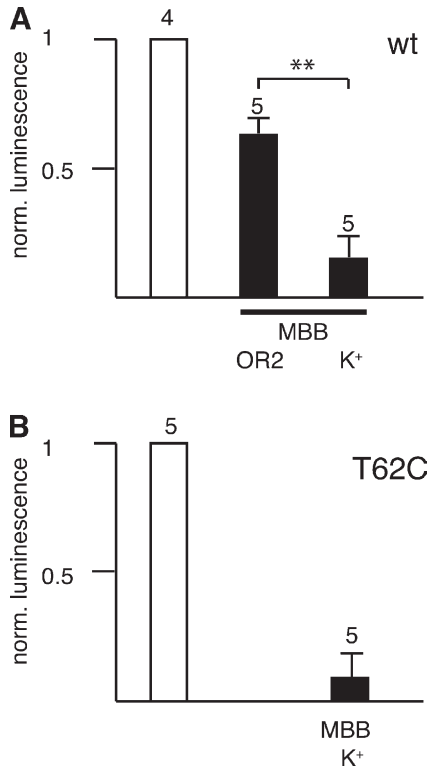

Figure 9. Effect of 1 mM MBB on ATP release from oocytes expressing wt Panx1 (A) and Panx1 T62C (B). Oocytes were preincubated with 150 mM KGlu for 10 min, and then transferred to fresh KGlu solution for a 10-min incubation period before ATP measurement in the supernatant (left column). MBB was included in the preincubation solution (right column). The middle column in A shows data for oocytes preincubated in OR2 containing MBB, and then transferred to KGlu solution. The means of ATP released from uninjected oocytes subjected to identical treatments were subtracted.

Another difference between MBB and MTSET reactions was observed in the TM3 segment, where only MTSET slightly inhibited conductance, whereas MBB had no detectable effect at all. MTSET may yield false positive results by a mechanism akin to the one described in the previous paragraph. Alternatively, a wide pore in this region may require multiple reactions with some or all of the six subunits of the channel. This may be feasible with the smaller MTS reagents but not with MBB. Regardless, the evidence for a contribution of TM3 to the pore lining remains weak. The fact that nonfunctional cysteine replacement mutants cluster in both TM1 and TM3 segments and the amino terminus of Panx1 indicates that minor perturbation of these segments can impair channel function. This could be from alteration of the permeation pathway as well as from effects on channel gating.

A gain of channel function at the resting membrane potential was observed for two mutant Panx1 channels, where the endogenous cysteines C346 and C40 were replaced by serines. These mutant channels lead to cell death, which could be prevented by CBX, a Panx1 channel inhibitor. These data indicate that the replacement of C40 or C346 leads to altered gating with preference for higher open probability and/or increased conductance.

A physiological function of Panx1 is to form an ATP release channel (Bao et al., 2004; Dahl and Locovei, 2006; Locovei et al., 2006a; Iglesias et al., 2009; Ransford et al., 2009). Here, we observed that ATP release from oocytes expressing wt Panx1, with its reactive terminal cysteine C426 or the mutant Panx1 T62C,C426S, was impaired by MBB. The inhibition of ATP release was most prominent if the oocytes were preincubated with MBB and the channels opened by high extracellular [K^+], indicating that MBB reached the cysteines through the open pore. ATP release and its inhibition were measured at a time point where the current inhibition had reached a steady-state level, yet the inhibition of ATP release exceeded that of current inhibition. This observation is consistent with a partial obstruction of the permeation pathway by the thiol reagent.

We thank Drs. K. Muller and H.P. Larsson for critically reading the manuscript.

This work was supported by the National Institutes of Health (grant GM48610).

Edward N. Pugh Jr. served as editor.

Submitted: 25 March 2010
Accepted: 20 September 2010

REFERENCES

Akabas, M.H., D.A. Stauffer, M. Xu, and A. Karlin. 1992. Acetylcholine receptor channel structure probed in cysteine-substitution mutants. *Science.* 258:307–310. doi:10.1126/science.1384130

Bao, L., S. Locovei, and G. Dahl. 2004. Pannexin membrane channels are mechanosensitive conduits for ATP. *FEBS Lett.* 572:65–68. doi:10.1016/j.febslet.2004.07.009

Bao, L., S. Samuels, S. Locovei, E.R. Macagno, K.J. Muller, and G. Dahl. 2007. Innexins form two types of channels. *FEBS Lett.* 581:5703–5708. doi:10.1016/j.febslet.2007.11.030

Bennett, M.V., L.C. Barrio, T.A. Bargiello, D.C. Spray, E. Hertzberg, and J.C. Sáez. 1991. Gap junctions: new tools, new answers, new questions. *Neuron.* 6:305–320. doi:10.1016/0896-6273(91)90241-Q

Boassa, D., C. Ambrosi, F. Qiu, G. Dahl, G. Gaietta, and G. Sosinsky. 2007. Pannexin1 channels contain a glycosylation site that targets the hexamer to the plasma membrane. *J. Biol. Chem.* 282:31733–31743. doi:10.1074/jbc.M702422200

Boassa, D., F. Qiu, G. Dahl, and G. Sosinsky. 2008. Trafficking dynamics of glycosylated pannexin 1 proteins. *Cell Commun. Adhes.* 15:119–132. doi:10.1080/15419060802013885

Bruzzone, R., S.G. Hormuzdi, M.T. Barbe, A. Herb, and H. Monyer. 2003. Pannexins, a family of gap junction proteins expressed in brain. *Proc. Natl. Acad. Sci. USA.* 100:13644–13649. doi:10.1073/pnas.2233464100

Bruzzone, R., M.T. Barbe, N.J. Jakob, and H. Monyer. 2005. Pharmacological properties of homomeric and heteromeric pannexin hemichannels expressed in Xenopus oocytes. *J. Neurochem.* 92:1033–1043. doi:10.1111/j.1471-4159.2004.02947.x

Chuang, C.F., M.K. Vanhoven, R.D. Fetter, V.K. Verselis, and C.I. Bargmann. 2007. An innexin-dependent cell network establishes left-right neuronal asymmetry in C. elegans. *Cell.* 129:787–799. doi:10.1016/j.cell.2007.02.052

Dahl, G. 1992. The Xenopus oocyte cell-cell channel assay for functional analysis of gap junction proteins. *In* Cell-Cell Interactions: A Practical Approach. B. Stevenson, W. Gallin, and D. Paul, editors. Oxford University Press, Oxford, UK. 143–165.

Dahl, G., and S. Locovei. 2006. Pannexin: to gap or not to gap, is that a question? *IUBMB Life.* 58:409–419. doi:10.1080/15216540600794526

Delmar, M., W. Coombs, P. Sorgen, H.S. Duffy, and S.M. Taffet. 2004. Structural bases for the chemical regulation of Connexin43 channels. *Cardiovasc. Res.* 62:268–275. doi:10.1016/j.cardiores.2003.12.030

Goodenough, D.A., D.L. Paul, and L. Jesaitis. 1988. Topological distribution of two connexin32 antigenic sites in intact and split rodent hepatocyte gap junctions. *J. Cell Biol.* 107:1817–1824. doi:10.1083/jcb.107.5.1817

Holmgren, M., Y. Liu, Y. Xu, and G. Yellen. 1996. On the use of thiol-modifying agents to determine channel topology. *Neuropharmacology.* 35:797–804. doi:10.1016/0028-3908(96)00129-3

Hu, X., and G. Dahl. 1999. Exchange of conductance and gating properties between gap junction hemichannels. *FEBS Lett.* 451:113–117. doi:10.1016/S0014-5793(99)00558-X

Hu, X., M. Ma, and G. Dahl. 2006. Conductance of connexin hemichannels segregates with the first transmembrane segment. *Biophys. J.* 90:140–150. doi:10.1529/biophysj.105.066373

Iglesias, R., G. Dahl, F. Qiu, D.C. Spray, and E. Scemes. 2009. Pannexin 1: the molecular substrate of astrocyte "hemichannels". *J. Neurosci.* 29:7092–7097. doi:10.1523/JNEUROSCI.6062-08.2009

Kaplan, R.S., J.A. Mayor, D. Brauer, R. Kotaria, D.E. Walters, and A.M. Dean. 2000. The yeast mitochondrial citrate transport protein. Probing the secondary structure of transmembrane domain iv and identification of residues that likely comprise a portion of the citrate translocation pathway. *J. Biol. Chem.* 275:12009–12016. doi:10.1074/jbc.275.16.12009

Kronengold, J., E.B. Trexler, F.F. Bukauskas, T.A. Bargiello, and V.K. Verselis. 2003. Single-channel SCAM identifies pore-lining residues in the first extracellular loop and first transmembrane domains of Cx46 hemichannels. *J. Gen. Physiol.* 122:389–405. doi:10.1085/jgp.200308861

Liu, Y., M.E. Jurman, and G. Yellen. 1996. Dynamic rearrangement of the outer mouth of a K+ channel during gating. *Neuron.* 16:859–867. doi:10.1016/S0896-6273(00)80106-3

Locovei, S., L. Bao, and G. Dahl. 2006a. Pannexin 1 in erythrocytes: function without a gap. *Proc. Natl. Acad. Sci. USA.* 103:7655–7659. doi:10.1073/pnas.0601037103

Locovei, S., J. Wang, and G. Dahl. 2006b. Activation of pannexin 1 channels by ATP through P2Y receptors and by cytoplasmic calcium. *FEBS Lett.* 580:239–244. doi:10.1016/j.febslet.2005.12.004

Locovei, S., E. Scemes, F. Qiu, D.C. Spray, and G. Dahl. 2007. Pannexin1 is part of the pore forming unit of the P2X(7) receptor death complex. *FEBS Lett.* 581:483–488. doi:10.1016/j.febslet.2006.12.056

Lü, Q., and C. Miller. 1995. Silver as a probe of pore-forming residues in a potassium channel. *Science.* 268:304–307. doi:10.1126/science.7716526

Ma, M., and G. Dahl. 2006. Cosegregation of permeability and single-channel conductance in chimeric connexins. *Biophys. J.* 90:151–163. doi:10.1529/biophysj.105.066381

Maeda, S., S. Nakagawa, M. Suga, E. Yamashita, A. Oshima, Y. Fujiyoshi, and T. Tsukihara. 2009. Structure of the connexin 26 gap junction channel at 3.5 Å resolution. *Nature.* 458:597–602. doi:10.1038/nature07869

Maroto, R., and O.P. Hamill. 2001. Brefeldin A block of integrin-dependent mechanosensitive ATP release from Xenopus oocytes reveals a novel mechanism of mechanotransduction. *J. Biol. Chem.* 276:23867–23872. doi:10.1074/jbc.M101500200

Oh, S., V.K. Verselis, and T.A. Bargiello. 2008. Charges dispersed over the permeation pathway determine the charge selectivity and conductance of a Cx32 chimeric hemichannel. *J. Physiol.* 586:2445–2461. doi:10.1113/jphysiol.2008.150805

Panchin, Y.V. 2005. Evolution of gap junction proteins—the pannexin alternative. *J. Exp. Biol.* 208:1415–1419. doi:10.1242/jeb.01547

Panchin, Y., I. Kelmanson, M. Matz, K. Lukyanov, N. Usman, and S. Lukyanov. 2000. A ubiquitous family of putative gap junction molecules. *Curr. Biol.* 10:R473–R474. doi:10.1016/S0960-9822(00)00576-5

Penuela, S., R. Bhalla, X.Q. Gong, K.N. Cowan, S.J. Celetti, B.J. Cowan, D. Bai, Q. Shao, and D.W. Laird. 2007. Pannexin 1 and pannexin 3 are glycoproteins that exhibit many distinct characteristics from the connexin family of gap junction proteins. *J. Cell Sci.* 120:3772–3783. doi:10.1242/jcs.009514

Pfahnl, A., and G. Dahl. 1998. Localization of a voltage gate in connexin46 gap junction hemichannels. *Biophys. J.* 75:2323–2331. doi:10.1016/S0006-3495(98)77676-3

Qiu, F., and G. Dahl. 2009. A permeant regulating its permeation pore: inhibition of pannexin 1 channels by ATP. *Am. J. Physiol. Cell Physiol.* 296:C250–C255. doi:10.1152/ajpcell.00433.2008

Rabadan-Diehl, C., G. Dahl, and R. Werner. 1994. A connexin-32 mutation associated with Charcot-Marie-Tooth disease does not affect channel formation in oocytes. *FEBS Lett.* 351:90–94. doi:10.1016/0014-5793(94)00819-1

Ransford, G.A., N. Fregien, F. Qiu, G. Dahl, G.E. Conner, and M. Salathe. 2009. Pannexin 1 contributes to ATP release in airway epithelia. *Am. J. Respir. Cell Mol. Biol.* 41:525–534. doi:10.1165/rcmb.2008-0367OC

Shi, L.B., and A.S. Verkman. 1996. Selected cysteine point mutations confer mercurial sensitivity to the mercurial-insensitive water channel MIWC/AQP-4. *Biochemistry.* 35:538–544. doi:10.1021/bi9520038

Silverman, W., S. Locovei, and G. Dahl. 2008. Probenecid, a gout remedy, inhibits pannexin 1 channels. *Am. J. Physiol. Cell Physiol.* 295:C761–C767. doi:10.1152/ajpcell.00227.2008

Silverman, W.R., J.P. de Rivero Vaccari, S. Locovei, F. Qiu, S.K. Carlsson, E. Scemes, R.W. Keane, and G. Dahl. 2009. The pannexin 1 channel activates the inflammasome in neurons and astrocytes. *J. Biol. Chem.* 284:18143–18151. doi:10.1074/jbc.M109.004804

Skerrett, I.M., J. Aronowitz, J.H. Shin, G. Cymes, E. Kasperek, F.L. Cao, and B.J. Nicholson. 2002. Identification of amino acid residues lining the pore of a gap junction channel. *J. Cell Biol.* 159:349–360. doi:10.1083/jcb.200207060

Trexler, E.B., M.V. Bennett, T.A. Bargiello, and V.K. Verselis. 1996. Voltage gating and permeation in a gap junction hemichannel. *Proc. Natl. Acad. Sci. USA.* 93:5836–5841. doi:10.1073/pnas.93.12.5836

Unwin, N. 1989. The structure of ion channels in membranes of excitable cells. *Neuron.* 3:665–676. doi:10.1016/0896-6273(89)90235-3

Wang, J., M. Ma, S. Locovei, R.W. Keane, and G. Dahl. 2007. Modulation of membrane channel currents by gap junction protein mimetic peptides: size matters. *Am. J. Physiol. Cell Physiol.* 293:C1112–C1119. doi:10.1152/ajpcell.00097.2007

Yen, M.R., and M.H. Saier Jr. 2007. Gap junctional proteins of animals: the innexin/pannexin superfamily. *Prog. Biophys. Mol. Biol.* 94:5–14. doi:10.1016/j.pbiomolbio.2007.03.006

Zhang, H., and A. Karlin. 1997. Identification of acetylcholine receptor channel-lining residues in the M1 segment of the beta-subunit. *Biochemistry.* 36:15856–15864. doi:10.1021/bi972357u

Zhou, X.W., A. Pfahnl, R. Werner, A. Hudder, A. Llanes, A. Luebke, and G. Dahl. 1997. Identification of a pore lining segment in gap junction hemichannels. *Biophys. J.* 72:1946–1953. doi:10.1016/S0006-3495(97)78840-4